Kramers potential study of the Rouse-like dynamics of short alkane chains

W. Paul[1] and H. L. Frisch[2]
[1]*Institut für Physik, Johannes-Gutenberg-Universität, Staudingerweg 7, D-55099 Mainz, Germany*
[2]*Department of Chemistry, The State University of New York at Albany, Albany, New York 12222*
(Received 10 July 1998)

In this work we present a Kramers potential study of the orientational dynamics and shear viscosity of short chain alkanes. In this approach the determination of the orientational relaxation time is reduced to the calculation of static moments of single chain conformations. We study a chemically realistic alkane model that asymptotically produces Gaussian chain conformations by means of a Monte Carlo simulation. Our results are applicable to single chain descriptions of polymer melt dynamics and to the intrinsic viscosity of molecules in a Θ solvent. When we map the unknown time unit of our relaxation time result for one particular chain length and temperature to the value obtained for the same parameters from a molecular dynamics simulation of a melt of these chains, we are able to reproduce the experimental data on the chain length dependence of the melt viscosity of alkane chains at this temperature. [S1063-651X(99)02207-2]

PACS number(s): 83.10.Nn, 02.70.Lq, 66.20.+d

I. INTRODUCTION

Following a suggestion made by Kramers [1], it is possible, at least for single chain polymer models, to obtain the low shear rate limit of the orientational relaxation time τ in a Rouse chain from biased sampling Monte Carlo computations of equilibrium radius of gyration data [2–4]. It turns out to lowest order in the shear rate $\dot{\gamma}$ that the shear flow can be replaced by its irrotational part, which is derivable from a velocity potential, and the calculation of the shear response can be reduced to the determination of the equlibrium radius of gyration of a chain under this potential streaming [2]. This then yields either the limiting intrinsic viscosity of such a model chain for which long range hydrodynamic forces are neglected or the Rouse model prediction of the melt viscosity of such chains. We apply this calculation procedure to a chemically realistic alkane model [5,6]. In the first version we only use the internal degrees of freedom of the model, and in the second version additionally the nonbonded interaction either only between pentad methylenes or also between 1-6 methylenes is included to prevent the overlap of these groups. Both versions, however, are *not* self-avoiding but random walks in their large scale structure, and are therefore models for polymer chains in a Θ solvent or in the melt. A complete specification of our model is given in Sec. II of this paper. We will look at the properties of these model chains as a function of chain length, especially in the region where the chains show considerable deviations from the limiting Gaussian behavior.

The technique has been applied previously to coarse-grained models of self-avoiding chains without internal degrees of freedom which where linear [2], circular [3] or branched [4]. On the other hand, polyethylene or alkanes have been extensively studied by computer simulations for many years, and in the last years the quality of the modeling has improved to a point where one can quantitativly predict static and dynamic properties of alkane melts [5–9]. Due to the large amount of computer time involved in such calculations, they are only able to cover short chains and/or high temperatures. It is therefore an intriguing question to what extent a single chain effective medium theory like the Kramers potential approach can reproduce and predict the shear response of these alkane chains in their Gaussian coiled state.

The basic theory of the Kramers potential approach is described in Refs. [2,4]. The biasing Kramers potential U_K acts on every monomer of the chains, with monomer positions measured from the center of mass of the chain. Thus for a point (x,y) the Kramers potential is

$$\frac{U_K}{k_BT}=\frac{1}{2}\frac{\zeta\dot{\gamma}xy}{k_BT}=gxy, \tag{1}$$

where ζ is the monomer friction coefficient. The only way the medium in which the chain moves enters into the model is this friction coefficient. Therefore, we can interpret our results either as describing a chain in a Θ solvent, where the friction is generated through the interaction with the solvent molecules, or a melt chain, the friction being produced by the interaction with the other chains in the melt. The latter application is usually not considered, but is based on the same physical devision into single chain response and background friction that is used in the Rouse treatment of polymer melt viscosity [10]: For this case one knows experimentally that the friction coefficient depends on temperature and chain length, so we can have $\zeta=\zeta(T,N)$ in Eq. (1). We denote a canonical average of a dynamical quantity E including this Kramers potential by $\langle E\rangle_g$ and let the usual equilibrium average where $g=0$ be denoted by $\langle E\rangle_0$. If X^2_{gyr} is the X component of the radius of gyration squared of our random walk chain, then the relaxation time τ^2 is given by

$$\tau^2=\lim_{g\to 0}\left[\frac{\langle X^2_{\mathrm{gyr}}\rangle_g}{\langle X^2_{\mathrm{gyr}}\rangle_0}-1\right]\Big/\, g^2. \tag{2}$$

By Taylor expanding the square bracket in Eq. (2) in powers of g one finds with N the number of repeat units in the chain and the coordinates given in the center of mass reference frame

TABLE I. Chemically realistic united atom force field used in the Monte Carlo generation of equlibrium chain conformations.

bond length	$l_{CC}=1.53$ Å $=$ const
bond angle	$U_\theta(\theta)=k^\theta/2(\cos\theta-\cos\theta_0)^2$
	$k^\theta=120$ kcal/mol, $\theta_0=110°$
dihedral angle	$\frac{1}{2}\sum_{n=1}^{3} k_n^\phi(1-\cos n\phi)$
	$k_1^\phi=1.5$ kcal/mol, $k_2^\phi=-0.764$ kcal/mol, $k_3^\phi=3.5$ kcal/mol
Lennard-Jones	$U_{LJ}(r_{ij})=\begin{cases}\epsilon_{\alpha\beta}\left[\left(\frac{\sigma}{r_{ij}}\right)^{12}-2\left(\frac{\sigma}{r_{ij}}\right)^{6}\right]-C & r_{ij}\leqslant 2\sigma \\ 0 & r_{ij}\leqslant 2\sigma\end{cases}$
	$\sigma=4.5$ Å, $\epsilon_{CH_2CH_2}=0.09344$ kcal/mol, $\epsilon_{CH_3CH_3}=0.22644$ kcal/mol,
	$\epsilon_{CH_3CH_2}=\sqrt{\epsilon_{CH_2CH_2}\epsilon_{CH_3CH_3}}$

$$\tau^2=\frac{1}{2}\left[\frac{1}{\langle X_{gyr}^2\rangle_0 N}\sum_{i=1}^{N}\sum_{j=1}^{N}\sum_{k=1}^{N}\langle x_i^2 x_j x_k y_j y_k\rangle_0 - \sum_{j=1}^{N}\sum_{k=1}^{N}\langle x_j x_k y_j y_k\rangle_0\right], \tag{3}$$

which shows that the dynamical entity τ^2 can be solely expressed in terms of equilibrium averaged static data for our random walk chains.

The first thing we shall check in our numerical calculations is the agreement in τ^2 calculated from either Eqs. (2) or (3), required by self-consistency. Besides varying the chain length N we will change the temperature of our Monte Carlo calculations, which affects the internal degrees of freedom in the chains. We will attempt to approximate a change in the screening of the excluded volume interactions either by changing the Θ solvent of a hypothetical infinitely dilute solution or changing the melt density, by changing the range of interactions between methylene units (in number of methylene units along the chain). This gives rise to the two versions of the model discussed earlier. Data on these changes of N, T and ''solvent quality'' and a comparison of our results with available experimental and computer simulation data on the viscosity of alkane chains will be presented in Sec. III. Finally we will present some conclusions in Sec. IV.

II. MODEL AND SIMULATION TECHNIQUE

In this work we apply the Kramers potential method to a chemically realistic model of polyethylene [5,6]. In this model the hydrogen atoms are not treated explicitly but are combined with the backbone carbons into one united atom. We will use the force field given in Table I. With this chemically realistic force field we now want to generate chain conformations which are representative for chains in the melt or in a Θ solvent. To do this we follow the procedure described in Refs. [11,12]. The probability for a chain conformation is given through its Boltzmann weight.

$$P(\{\vec{r}_i\})=\frac{1}{Z}\exp\left\{-\beta\left[\sum_{i=1}^{N-1}U_l(l_i)+\sum_{i=1}^{N-2}U_\theta(\theta_i)+\sum_{i=1}^{N-3}U_\phi(\phi_i)+\frac{1}{2}\sum_{i,j=1}^{N}U_{LJ}(r_{ij})\right]\right\}, \tag{4}$$

where $\beta=1/k_BT$, and we have formally included a potential-energy term for the bond length which in the actual calculation will be taken as a constant. The first three terms are expressed in the internal coordinates of a chain (bond lengths, bond angles, and dihedral angles) whereas the last nonbonded term depends on the space coordinates of the particles and thereby for each monomer pair (i,j) on all internal degrees of freedom between them. If the nonbonded term is absent, the probability factorizes as

$$P(\{\vec{r}_i\})=\frac{1}{Z}\prod_{i=1}^{N-1}e^{-\beta U_l(l_i)}\prod_{i=1}^{N-2}e^{-\beta U_\theta(\theta_i)}\prod_{i=1}^{N-3}e^{-\beta U_\phi(\phi_i)}. \tag{5}$$

To determine the partition function of the chain as the integral over the configuration space of the internal coordinates, we can proceed by a simple importance sampling Monte Carlo scheme, building up the chain by choosing each individual degree of freedom according to its own probability distribution:

$$P(l_i)=\frac{e^{-\beta U_l(l_i)}}{\int_0^\infty dl_i e^{-\beta U_l(l_i)}}, \tag{6}$$

$$P(\theta_i)=\frac{e^{-\beta U_\theta(\theta_i)}}{\int_0^\pi d\theta_i e^{-\beta U_\theta(\theta_i)}},$$

$$P(\phi_i)=\frac{e^{-\beta U_\phi(\phi_i)}}{\int_0^{2\pi} d\phi_i e^{-\beta U_\phi(\phi_i)}}.$$

This reduces all thermodynamic averages to the calculations of arithmetic sample averages over the set of chains we generate. We will study this simplified model without any nonbonded interaction as a test and benchmark case for the Kramers potential approach to chemically realistic polymer models. For this case we will generate 10^7 independent chains of length $N=200$. Discarding chain end effects we can simultanously sample the properties of all chains with length $N<200$ by this procedure.

If we want to model alkane chains in a melt or in a Θ solvent we will have to include the Lennard-Jones interactions. However, we cannot simply include them between all monomers in the chain [12] because this would lead to either large scale self-avoiding walk statistics (good solvent, high temperatures) or to a collapsed globular state (bad solvent, low temperatures), neither of which would be representative of the melt or Θ solvent we wish to describe. To achieve a large scale random walk structure one has to neglect the Lennard-Jones interactions between monomers beyond a certain chemical distance of these monomers along the chain, irrespective of their distance in space. The most pronounced effect here is the so called pentane effect, generated by the inclusion of the Lennard-Jones interaction between monomers which are four bonds apart along the chain, i.e. 1-5, 2-6, . . . [12]. Including this interaction removes $(\text{gauche})^+(\text{gauche})^-$ (g^+g^-) configurations of adjacent dihedral angles from the chain conformation, which would lead to a strong overlap of monomers 1-5, etc. This interdependence of successive dihedral angles has to be included in successful rotational isomeric state (RIS) modeling of polyethylene [13], and was shown in Ref. [14] to reproduce the large scale conformation of $C_{100}H_{202}$ melt chains at high temperatures. To determine the effect of the chemical cutoff distance for the Lennard-Jones interaction, we will additionally study the case where 1-5 and 1-6 interactions are included.

With the inclusion of the Lennard-Jones interaction we can no longer generate a chain according to its correct Boltzmann weight. Let us denote a thermodynamic average without the Lennard-Jones interaction as $\langle A\rangle_0$ and one with the Lennard-Jones interaction as $\langle A\rangle_{\mathrm{LJ}}$. Then we have

$$\langle A\rangle_{\mathrm{LJ}}=\frac{\langle Ae^{-\beta U_{\mathrm{LJ}}}\rangle_0}{\langle e^{-\beta U_{\mathrm{LJ}}}\rangle_0}. \tag{7}$$

To determine averages in the case with the Lennard-Jones interaction, we therefore have to weigh all configurations that we generated by the above described treatment of the internal degrees of freedom by the Boltzmann factor of the nonbonded interaction. The term $\langle\exp\{-\beta U_{\mathrm{LJ}}\}\rangle_0(N,T)$ describes the attrition, i.e., by which factor the relative weight of chains of length N at a temperature T is reduced for each chain we try to generate. This factor decreases exponentially with chain length, and it is about 10^{-4} for chains of length $N=80$ and the inclusion of the 1-5 Lennard-Jones interaction at the temperatures we want to study. This means that for that 10^7 chains we generate we only obtain the statistical weight equivalent to 10^3 chains for those of length $N=80$, thus limiting the chain lengths we can study with the inclusion of the nonbonded interaction. In Sec. III we will discuss

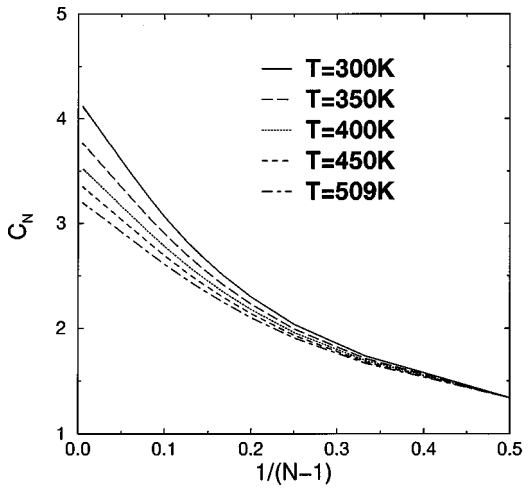

FIG. 1. Chain length dependence of the characteristic ratio of the chains (for a definition, see text) for several temperatures indicated in the legend and the version of the model where no Lennard-Jones interactions are included.

static and dynamic properties for the cases with and without nonbonded interactions at the temperatures $T=300$ K, 350 K, 400 K, 450 K and 509 K.

III. RESULTS

In the case without inclusion of Lennard-Jones interactions we generated data with high statistical accuracy for chains up to length $N=200$. As an example of the behavior of the large scale static properties of the chains, in Fig. 1 we display the characteristic ratio of the chains, defined as $C_N=\langle R^2\rangle/(N-1)l^2$ where $\langle R^2\rangle$ is the mean squared end-to-end distance of the chains, and $l=1.53$ Å is the C—C bond length, as a function of inverse chain length (number of C—C bonds). The curves for the different temperatures merge on the scale of the trimer since the bond angle force constant is of the order of 60 000 K, so that the temperature variation we performed has no influence on the size of the trimer. For $N\to\infty$ the characteristic ratio approaches a temperature dependent limiting value C_∞, and the leading correction is linear in the chain length [13]. For chain lengths $N>20$ we can perform linear regressions to extract the C_∞ values. This procedure still works for the case with inclusion of the Lennard-Jones interactions, where we can use a range of chain lengths $N=20$ to $N\approx 70$ where we have sufficient statistical accuracy for the regression analysis. The result of this analysis is displayed in Fig. 2, where we show the extrapolated values of C_∞ as a function of temperature for the three versions of the model we studied. It is obvious from this figure that there is a large effect due to the inclusion of the pentad Lennard-Jones interaction which removes the $(\text{gauche})^+$–$(\text{gauche})^-$ conformations of consecutive dihedral angles and increases the chain stiffness by a factor of 2. This was also observed in an earlier study of the equilibrium size of alkane chains using realistic potentials [12]. The inclusion of the 1-6 interaction in addition to the 1-5 interaction introduces an additional net attraction between the monomers into the model, and leads to a slight decrease of the chain stiffness. A further extension of the Lennard-Jones interaction along the chain would increase this effect [12].

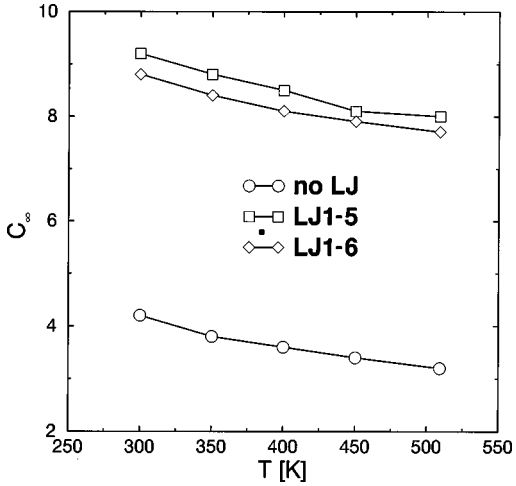

FIG. 2. Extrapolated infinite chain length characteristic ratio as a function temperature. Connected circles are for the case without Lennard-Jones interactions, connected squares for the inclusion of the pentane 1-5 interaction, and connected diamonds for the further inclusion of the 1-6 interaction.

We will address the question which of the model versions best represents alkane chains in the melt state at a later point in the manuscript.

First let us turn to the determination of the dynamic properties of the chains using the Kramers potential. From Eq. (3) we can determine the rotational (end-to-end vector) relaxation time of the molecules solely through the evaluation of sixth and fourth order static moments of the chain conformation. The result of this analysis in the case without any Lennard-Jones interaction is shown in Fig. 3. The relaxation times are normalized to the expected asymptotic Rouse scaling law $\tau \propto N^2$. For the different temperatures we see a slow approach to this behavior as a function of chain length. For the analysis of the cases with Lennard-Jones interactions it is important to note that for chain lengths $N<100$ we see significant corrections to the aysmptotic Rouse prediction. To address the question of consistency between the two methods [Eqs. (2) and (3)] to determine the relaxation time of the molecules, we have to look into the dependence of the average squared radius of gyration on the strength of the shear flow as parametrized through the parameter g in the Kramers potential [cf. Eq. (1)]. In Fig. 4 we show the Kramers-averaged squared radius of gyration as a function of g^2. According to Eq. (2) there should be a linear variation in this plot for small g^2 values, which is indeed what is observed. The dashed lines are fits of the form $R_G^2(g)=R_G^2(0)+cg^2$. The range of shear strengths for which this linear variation is observable decreases with increasing chain length. Furthermore, the value of the Kramers-averaged squared radius of gyration in this g^2 regime is only slightly different from the equilibrium value for $g=0$ displayed in the figure by the open triangles. From this figure it is evident that the use of Eq. (2) for the determination of the relaxation time of the chains requires a calculation of the Kramers-averaged gyration radii with high statistical accuracy to be able to determine the slope of the curves in Fig. 4 through a regression analysis. As an example of this analysis we show the result for $T=509$ K in Fig. 5(a). The full curve is the relaxation time determined from the moments, and the dashed and somewhat noisy curve is the result of the analysis of Eq. (2). For $N>30$ we obtain a perfect agreement between the two methods, but for $N<30$ the moment method is superior since the fit method is hampered by the very small effect the shear flow has on the extension of these small chains, making the Kramers-averaged radius of gyration almost indistinguishable from the equilibrium one. We can put that differently by saying that, in order to determine the relaxation time from the effect of the shear flow on the average radius of gyration, we would have to go to much higher shear rates for chains of length $N<30$ in order to resolve the difference between the situations with and without flow. The moment method, on

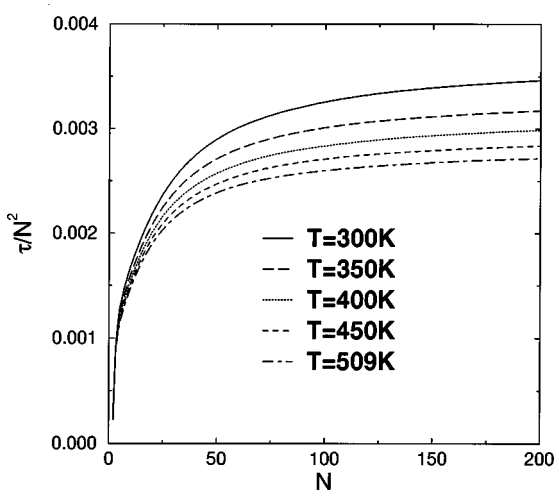

FIG. 3. End-to-end vector orientational correlation time as a function of chain length, as obtained from the moment equation for the case of no Lennard-Jones interactions. The curves are for the different temperatures denoted in the legend. The relaxation time is scaled with the asymptotic power law dependence of the Rouse theory.

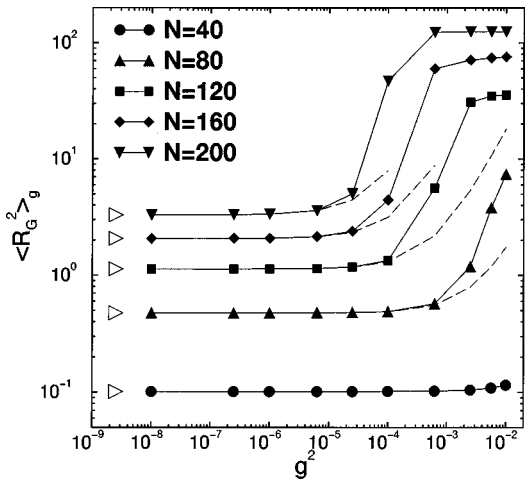

FIG. 4. Dependence of the Kramers-averaged mean squared radius of gyration of the molecules on the scaled Kramers potential strength [see Eq. (1)]. The curves are for different chain lengths indicated in the legend and the case without any Lennard-Jones interactions for $T=300$ K. The regime where Eq. (2) can be used to determine the relaxation time is the linear portion of these curves. The open triangles indicate the zero shear rate ($g=0$) value of the mean squared radius of gyration.

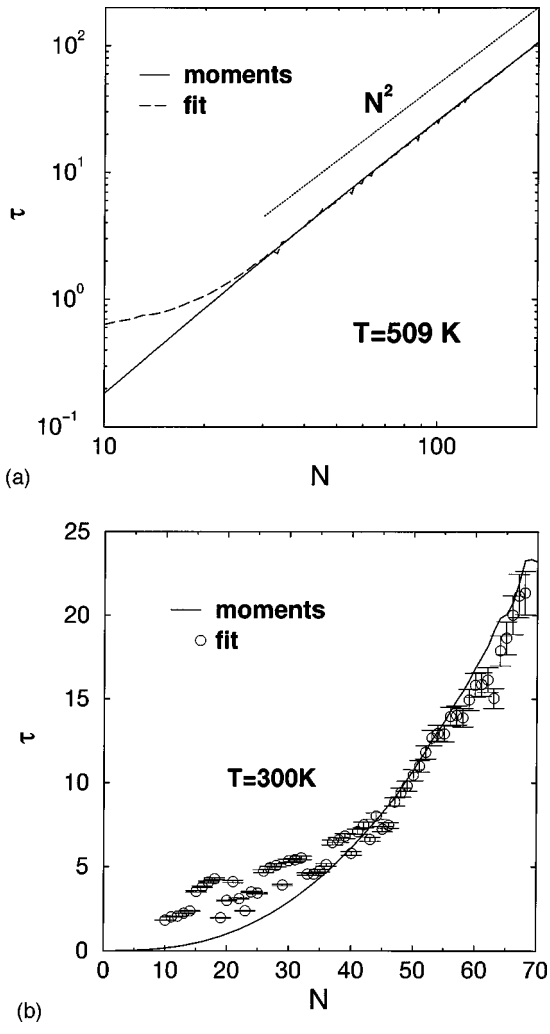

FIG. 5. Comparison of the results for the relaxtion time obtained from the moment equation (3) and the fit equation (2): (a) no Lennard-Jones interaction; (b) 1-5 Lennard-Jones interaction included. The temperatures are given in the figures.

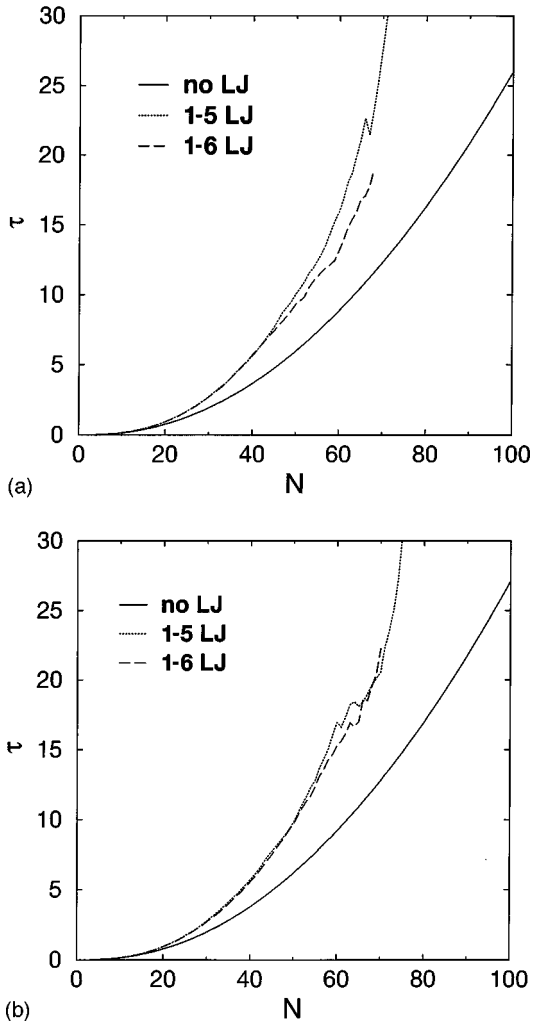

FIG. 6. Influence of the inclusion of the Lennard-Jones interaction on the relaxtion time as obtained from the moment equation: (a) 509 K and (b) 450 K.

the other hand, looks at higher moments of the gyration radius distribution which are more sensitive to the strength of the flow, and therefore gives more reliable data in the short chain region. For comparison we have included the Rouse N^2 behavior for large N as the dotted line in the figure. In the cases with Lennard-Jones interactions the fit method still works, albeit with a large systematic uncertainty due to the very much reduced statistical quality of the available data. Figure 5(b) shows the result for $T=300$ K, and we now include the error bars for the fitted relaxation time data. For small N the fitted values are again larger than the moment values, but for $35<N<65$ we can see a reasonable agreement between the two methods. On the whole, however, it is preferable to use the moment equation (3) for the determination of the longest relaxation time of the molecules.

Same as for the static properties, the inclusion of Lennard-Jones interactions has a significant influence on the relaxation time. The relaxation time for the stiffer chains, where the Lennard-Jones interaction is included are much larger than those in the case without Lennard-Jones interactions and the difference between the two increases with increasing chain length [Figs. 6(a) and 6(b)]. In Fig. 6(a), which shows the behavior for $T=509$ K, there is a slight decrease of the relaxation time for the chain lengths we were able to study when we go from the 1-5 Lennard-Jones case to the 1-6 Lennard-Jones case, which also showed a small decrease in chain stiffness. For $T=450$ K, however, we cannot make out any difference between the two cases for the chain lengths we were able to study, and the curves agree within their statistical errors which can be deduced from the noisiness of the curves.

At this point we can conclude that we are able to determine the longest relaxation time of alkane chains up to lengths about $N=70$ using the Kramers potential approach. Since the model we are using is a chemically realistic model for the alkane chains, the static properties we obtain are directly given in experimental units. The model has also been used in extensive molecular dynamics simulations of the static and dynamic properties of alkane chain melts [5,6,9] for chains of length up to $N=100$. It was shown to reproduce the experimental information on the size of the chains in the melt [6]. Therefore we can use the available molecular dynamics (MD) data to determine which cutoff in the Lennard-Jones interaction corresponds to the excluded volume screening the chains feel in a melt situation. This correspondence

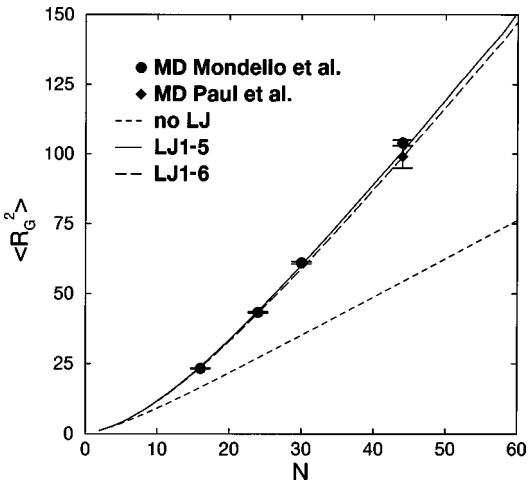

FIG. 7. Equilibrium value of the mean squared radius of gyration as a function of chain length for $T=400$ K. The filled symbols are from two MD simulations of melts of the respective chain length using the same chemically realistic model we employ here. The curves are the result of a Monte Carlo sampling of single chain conformations using either no Lennard-Jones interaction (dashed curve), only the 1-5 interaction (full curve), or the 1-5 and 1-6 interaction (long-dashed curve). The inclusion of only the 1-5 Lennard-Jones interaction seems to compare best to the excluded volume screening situation in the alkane melts.

cannot be deduced *a priori* from the microscopic model, and it depends on the polymer species under study and through the excluded volume screening length in the melt it strongly depends on melt density. In Fig. 7 we show our single chain Monte Carlo results for the mean squared average radius of gyration at 400 K for the three versions of our model and compare these to the results of MD simulations by Mondello *et al.* and Paul, Smith, and Yoon. Mondello *et al.* looked at the chain length dependence of the mean squared radius of gyration of alkane chains in the melt for three different chemically realistic alkane models, including the one one of us proposed earlier [5]. For $N=44$ their result agrees within the error bars with the one Paul, Smith, and Yoon [5] reported. For the range of chain lengths displayed in Fig. 7 we conclude that both the 1-5 and 1-6 Lennard-Jones cases are able to reproduce the MD data (note that these are all direct simulation results and there is no fitting envolved). The 1-6 case, however, for larger chain lengths seems to increase less strongly than the 1-5 case and the MD data. We therefore conclude that the 1-5 Lennard-Jones version of our model is able to reproduce the static conformations of short alkane melt chains at 400 K. This is further supported by an analysis of the characteristic ratio for this case as a function of chain length using the same asymptotic relation as for Fig. 2,

$$C_N(T)=C_\infty(T)-\frac{c}{N}. \tag{8}$$

We obtain $C_N(400)=8.5-53.3/N$, $C_N(450)=8.1-48.2/N$, and $C_N(509)=8.0-48.5/N$. So we have $C_{N=44}(400)=7.3$, which agrees with the result of Refs. [5,9], $C_{N=44}(450)=7.0$ compared to 7.1 of Ref. [5] and $C_{N=100}(509)=7.5$ compared to 7.2 of Ref. [6]. From the temperature dependence of the radius of gyration for a fixed chain length, we can furthermore deduce the temperature coefficient of the chains:

$$\kappa=\frac{d\ln(\langle R_G^2\rangle)}{dT}. \tag{9}$$

Following Ref. [15] we perform a linear fit to $\langle R_G^2\rangle^{1/2}$ as a function of temperature for 300 K$<T<$509 K, and average the resulting small temperature dependence of κ. Our results are $\kappa=-1.2\times10^{-3}$ K^{-1} for $N=60$ and $\kappa=-1.1\times10^{-3}$ K^{-1} for $N=44$, which are in good agreement with the experimental results of Ref. [15] of $\kappa=-(1.06\pm0.07)\times10^{-3}$ K^{-1} for a polyethylene of weight average molecular weight $M_w=32000$ g/mol and $\kappa=-(1.25\pm0.06)\times10^{-3}$ K^{-1} for a polyethylene of weight average molecular weight $M_w=53\,000$ g/mol.

Having established that the 1-5 Lennard-Jones case describes alkane chains in the melt, we can now try to analyze the predictions for the relaxation time we obtain from our model. For this purpose we have to note that our results are given in dimensionless units (g), and we have to determine our underlying time scale by matching our result for the end-to-end vector orientational correlation time again to results of MD simulations using the same model. Paul, Smith, and Yoon [5] reported a relaxation time for the end-to-end vector for C_{44} at 450 K of $\tau_{\mathrm{MD}}=494$ ps. We obtain $\tau=3.303$ for the case without Lennard-Jones interaction, and $\tau=5.204$ for the 1-5 case. Since the 1-6 case gave results that were indistinguishable from the 1-5 case at the temperatures of interest, we will not discuss it further. Equating the relaxation times results in a time unit of $1\,\tau=150$ ps without Lennard-Jones interaction and $1\,\tau=95$ ps with the Lennard-Jones interaction. Mondello *et al.* also showed that one can reproduce dynamic shear viscosity data as obtained from a nonequilibrium molecular dynamics simulation using equilibrium data for the orientational correlation time of the molecules. In the Rouse model the shear viscosity can be calculated from this relaxation time by

$$\eta=\frac{\pi^2\rho N_A k_B T\tau}{12M}, \tag{10}$$

where ρ is the mass density, N_A is Avogadro's number, k_B is Boltzmann's constant, and M is the molar mass of the molecule. This relation also gave the correct viscosity prediction for small chain lengths $N<60$, where the Rouse model is not a consistent description of the chain dynamics. For small alkane chains in the melt there is an experimental set of data in the literature for densities and shear viscosities for several chain lengths at $T=450$ K [16]. Using the densities they reported, we can calculate our prediction for the shear viscosities of these alkane melts using the time scaling performed above. In Fig. 8 we show the result of this approach for different chain lengths. The full line is the prediction from the 1-5 Lennard-Jones case, and the dashed line the predicion for no Lennard-Jones interactions. Both have to agree for C_{44} by construction but their chain length dependence is very different. Also included are the experimental data of Pearson *et al.*, which exactly agree with the prediction for the 1-5 case. This again shows the applicability of

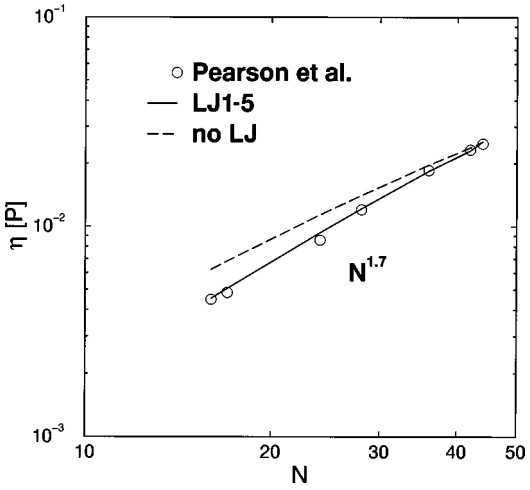

FIG. 8. Comparison of the alkane melt viscosity as determined from the Kramers potential relaxation times with experimental data of Pearson *et al.* at 450 K. After mapping of the unknown Kramers time scale to results of MD simulations for a C_{44} melt, the Kramers prediction for the viscosity in the 1-5 Lennard-Jones case exactly agrees with the experimental data. The viscosity scales as $N^{1.7}$, which compares well with the $N^{1.8}$ behavior that Pearson *et al.* reported for unentangled alkanes in the melt.

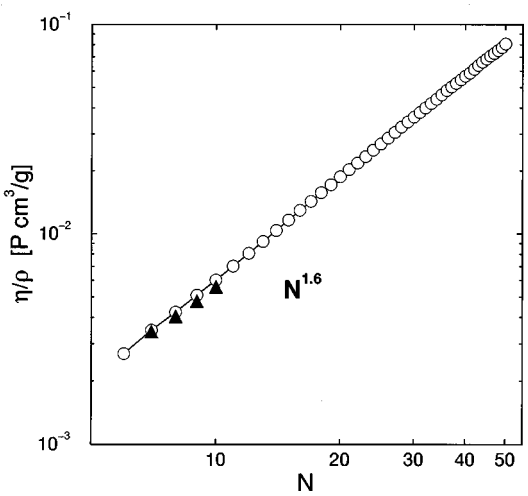

FIG. 9. Predicted kinematic viscosity (open circles) as a function of chain length for alkane melts at 400 K. The kinematic viscosity is predicted to show a $N^{1.6}$ behavior at this temperature. The filled triangles are measured kinematic viscosities of short paraffins at $T=372$ K (from Ref. [18]).

Eq. (10) for relating the longest relaxation time of the molecule to the shear viscosity. More astonishingly this figure shows that through the Kramers approach we are able to predict correctly the chain length dependence of experimental shear viscosity data by means of the calculation of purely static conformational averages of the chains (the relaxation times were determined through the moment equation). From our calculation we would determine a behavior $\eta \propto N^{1.7}$, which agrees within the uncertainties with the $N^{1.8}$ behavior Pearson *et al.* reported. Both results differ from the Rouse prediction $\eta \propto N$ due to the chain end effects on the monomer friction coefficient not accounted for in the Rouse model (the chain length dependence of the density is weak: $\rho \propto N^{0.1}$).

At this point we should note that the approach is, however, not capable of also reproducing the temperature dependence of the relaxation times (viscosities) with just the single time scaling. At $T=400$ K, Paul, Smith, and Yoon [5] reported an orientational correlation time of $\tau_{\mathrm{MD}}=938$ ps (which is almost twice as large as for $T=450$ K), whereas the Kramers result is $\tau=5.298$ (which is only slightly larger than for 450 K). The reason for this difference is that for short alkane chains, which show an Arrhenius behavior of the viscosity up to their crystallization temperature) the actual relaxation time of the chains is mainly determined by the temperature dependence of the local mobility which is given by a thermally activated crossing of the barriers between the trans and the gauche states in the dihedral angle potential. In contrast the moments that enter the Kramers calculation are not susceptible to the barriers in this potential but to the energetic difference between the trans and gauche minima. This approach is therefore not able to predict the temperature dependence of the relaxation times correctly using just one fixed translation of the time scale. At each temperature one has to perform the time scaling seperately for a chain length where independent information on the orientational correlation times is available. As a last point we will use this approach at $T=400$ K to predict the kinematic viscosity as a function of chain length. Equating the above cited values for the relaxation time as obtained from MD and the Kramers approach we obtain a time unit $1\tau=177$ ps. The results for the kinematic viscosity as a function of chain length at $T=400$ K are displayed in Fig. 9. From this calculation the kinematic viscosity of alkane melt chains at $T=400$ K should scale as $N^{1.6}$ for $6<N<50$. We also include kinematic viscosity data reported in Ref. [17] for short chain paraffins. We can see that the agreement is almost quantitative; however, the experimental data seem to show a slightly smaller effective exponent as a function of chain length in the experimentally reported range.

IV. CONCLUSIONS AND OUTLOOK

We showed in Sec. III that the Kramers potential approach that reduces the determination of the shear response of molecules to the calculation of static moments of the single chain conformations can be successfully and consistently applied to a chemically realistic alkane chain model. Comparing to results for the mean squared radius of gyration from MD simulations of melts of short alkane chains, which had employed the same realistic force field that we are using, we concluded that the truncation of the Lennard-Jones interaction beyond the pentane 1-5 distance corresponds to the excluded volume screening conditions in the alkane melts. The Kramers approach results in values for the orientational autocorrelation time of the molecules given in units of a scaled shear response time that includes the *a priori* unknown monomer friction coefficient. To translate the Kramers relaxation times into real time units, we mapped our result for the relaxation time of C_{44} at 450 K to the result obtained for this relaxation time from a MD simulation of a melt of these chains at the same temperature that had used the same realistic force field. With this time scale identification and the Rouse formula connecting the melt shear viscosity to the orientational correlation time, we were able to re-

produce the experimental chain length dependence of the shear viscosity of short chain alkane melts at 450 K.

This shows that the chain length dependence of the melt viscosity for short chains can be predicted on grounds of a purely static calculation of moments of single chain conformations. The approach fails, however, in the prediction of the temperature dependence of the viscosity. The reason for this is that the temperature dependence is to a large degree determined by the temperature dependence of the main local conformational relaxation mechanism, which is the activated crossing of the barriers in the torsion potential. (This assumes that intermolecular packing effects that eventually lead to a glass transition of the melt are not important, as is the case for the short alkanes that we studied.) A sampling of equilibrium conformations, however, is only susceptible to the energy difference between the minima in this potential, and cannot capture the effect of the barriers. Therefore, the time mapping between the Kramers results and experimental or MD simulation data on the relaxation time has to be done for each temperature seperately.

The application of our results to the calculation of the intrinsic viscosity of alkane chains in a Θ solvent is straightforward. The intrinsic viscosity can be defined as [18] the limit (for small shears), and as the number density n of chains in solution approaches zero of

$$\left(\frac{105}{16}\right)^{1/2}\frac{k_B T\tau}{\eta_s}=\frac{\eta-\eta_s}{n\eta_s}, \tag{11}$$

where η is the viscosity of the solution and η_s is the viscosity of the solvent. This has been studied for coarse-grained models of linear chains, rings and stars with excluded volume interactions but no Lennard-Jones interaction [2–4]. In Ref. [2] it was also shown how to include hydrodynamic forces on the level of the preaveraged Oseen tensor into this approach. A comparison of Eq. (11) with experimental data for alkanes in Θ solvents has to await a suitably large base of experimental alkane intrinsic viscosity data.

ACKNOWLEDGMENTS

One of us (H.L.F.) acknowledges support by the Guggenheim Foundation and the NSF under Grant No. DMR9628224. It is a pleasure to thank G. D. Smith for helpful comments.

[1] H.A. Kramers, J. Chem. Phys. **14**, 615 (1946).
[2] H.L. Frisch, N. Pistoor, A. Sariban, K. Binder, and S. Fresjan, J. Chem. Phys. **89**, 5194 (1988).
[3] S. Sharma, M. Schulz, and H.L. Frisch, Comput. Polym. Sci. **4**, 13 (1994).
[4] K. Ohno, M. Schulz, K. Binder, and H.L. Frisch, J. Chem. Phys. **101**, 4452 (1994).
[5] W. Paul, G.D. Smith, and D.Y. Yoon, J. Chem. Phys. **103**, 7156 (1995).
[6] W. Paul, G.D. Smith, and D.Y. Yoon, Macromolecules **30**, 7772 (1997); G.D. Smith, W. Paul, D.Y. Yoon, A. Zirkel, J. Hendricks, D. Richter, and H. Schober, J. Chem. Phys. **107**, 4751 (1997); W. Paul, G.D. Smith, D.Y. Yoon, B. Farago, S. Rathgeber, A. Zirkel, L. Willner, and D. Richter, Phys. Rev. Lett. **80**, 2346 (1998).
[7] G.D. Smith and D.Y. Yoon, J. Chem. Phys. **100**, 649 (1994); G.D. Smith, D.Y. Yoon, W. Zhu, and M. Ediger, Macromolecules **28**, 5897 (1995).
[8] J.I. Siepmann, S. Karaborni, and B. Smit, Nature (London) **365**, 330 (1993).
[9] M. Mondello and G.S. Grest, J. Chem. Phys. **106**, 9327 (1997); M. Mondello, G.S. Grest, E.B. Webb III, and P. Peczak, J. Chem. Phys. **109**, 798 (1998).
[10] M. Doi and S.F. Edwards, *The Theory of Polymer Dynamics* (Clarendon Press, Oxford, 1986).
[11] J. Baschnagel, K. Binder, W. Paul, M. Laso, U.W. Suter, I. Batoulis, W. Jilge, and T. Bürger, J. Chem. Phys. **95**, 6014 (1991).
[12] J. Baschnagel, K. Quin, W. Paul, and K. Binder, Macromolecules **25**, 3117 (1992).
[13] P.J. Flory, *Statistical Mechanics of Macromolecules* (Hanser, Munich, 1988).
[14] J. Han, R.L. Jaffe, and D.Y. Yoon, Macromolecules **30**, 7245 (1997).
[15] A.T. Boothroyd, A.R. Rennie, and C.B. Boothroyd, Europhys. Lett. **15**, 715 (1991).
[16] D.S. Pearson, G. Ver Strate, E. Von Meerwall, and F.C. Schilling, Macromolecules **20**, 1133 (1987).
[17] American Petroleum Institute Research Project 44, in *Physical Constants of Hydrocarbons* (American Society for Testing and Materials, Philadelphia, 1971).
[18] R.B. Bird, C.F. Curtiss, R.C. Armstrong, and O. Hassager, *Dynamics of Polymeric Liquids*, 2nd ed. (Wiley, New York, 1987), Vol. 2, Chap. 15.